

Synchrotron-based highest resolution FTIR spectroscopy of chlorobenzene



Sieghard Albert^{a,b,*}, Karen Keppler^a, Philippe Lerch^b, Martin Quack^{a,*}, Alexander Wokaun^c

^aPhysical Chemistry, ETH Zurich, CH-8093 Zurich, Switzerland

^bSwiss Light Source, Paul-Scherrer-Institute, CH-5232 Villigen, Switzerland

^cEnergy Research Department, Paul-Scherrer-Institute, CH-5232 Villigen, Switzerland

ARTICLE INFO

Article history:

Received 10 February 2015

In revised form 2 March 2015

Available online 18 March 2015

Keywords:

Synchrotron

FTIR spectroscopy

High resolution spectroscopy

Infrared

Isotopes

Chlorobenzene

Pollutants

ABSTRACT

We report the Fourier Transform Infrared (FTIR) spectrum of chlorobenzene (C_6H_5Cl) measured using synchrotron radiation and the ETH-SLS 2009 prototype spectrometer at the Swiss Light Source (SLS). The maximum optical path difference of these measurements was 11.8 m leading to a resolution of better than 0.0008 cm^{-1} . The spectra were taken at room temperature in the range $600\text{--}900\text{ cm}^{-1}$. It was possible to analyze the in-plane mode ν_{12} of A_1 symmetry ($\tilde{\nu}_0 = 706.6686\text{ cm}^{-1}$) and the out-of-plane mode ν_{10b} of B_1 symmetry ($\tilde{\nu}_0 = 741.2240\text{ cm}^{-1}$) of $C_6H_5^{35}Cl$. In addition, the ground state constant Δ_K of $C_6H_5^{35}Cl$ has been readjusted using combination differences (CD).

© 2015 Elsevier Inc. All rights reserved.

1. Introduction

The use of synchrotron radiation sources has greatly enhanced the possibilities of highest resolution Fourier Transform Infrared spectroscopy of polyatomic molecules [1–11]. In recent work we have shown that the infrared spectra of molecules as complex as naphthalene [3], azulene [8] and indene [10] can be rotationally resolved and analyzed, which can help the search for the spectra of such molecules in an astrophysical context. Furthermore tunneling dynamics in excited vibrational states of aromatic molecules such as phenol isotopomers can be studied successfully [7]. Even the spectra of moderately complex chiral molecules such as CDBrClF and CHBrF and others have been analyzed successfully [9,11] which provides a starting point for their use in experiments on molecular parity violation [12] which relates to some of the most fundamental current questions on molecular and biomolecular structure and dynamics [13–15].

Further important questions can be addressed by the study of molecules important for the spectroscopy of the Earth's atmosphere [16–24]. In the past, much high resolution spectroscopic work has concentrated on relatively simple atmospheric trace

gases such as ozone [18], methane [20–24] or some of the simpler fluoro-chloro-hydrocarbons [25], to name just a few selected examples from a very large body of work usually based on FTIR spectroscopy with conventional light sources.

Synchrotron-based FTIR spectroscopy allows us now to study more complex pollutants such as chlorobenzene, which is the subject of our present investigation. Chlorobenzene is a precursor of the polychlorinated biphenyls (PCB) [31] and tetrachlorodibenzo-1,4-dioxin [32] (TCDD) produced in industrial processes. Both compounds are extremely toxic for the environment. They can be generated by combustion of chlorinated benzenes. To gain more insight into such processes we have started to study the prototypical chlorinated aromatic compound chlorobenzene C_6H_5Cl [33] using high resolution FTIR spectroscopy in combination with synchrotron light. The vibrational spectrum of chlorobenzene (C_6H_5Cl) was assigned in [34–37]. Although benzene and monodeutero benzene have been studied at high resolution, including work from our group [38–40] and recent progress has been made in the analysis of the substituted aromatic molecules phenol [7] and fluorobenzene [33,41], there existed so far only one rovibrational analysis of the ν_{19a} band of chlorobenzene from [42] using diode laser jet spectroscopy. The vibrational ground state has been analyzed using submm wave spectroscopy in [43].

Chlorobenzene, (C_6H_5Cl), is a molecule of C_{2v} symmetry. The coordinate system was chosen as shown in Fig. 1 so that the

* Corresponding authors at: Physical Chemistry, ETH Zurich, CH-8093 Zurich, Switzerland.

E-mail addresses: albert@ir.phys.chem.ethz.ch (S. Albert), martin@quack.ch (M. Quack).

twofold rotational axis, the z -axis, goes through the Cl atom, the y -axis lies perpendicular to z in the plane of the molecule, and the x -axis intersects the center of gravity perpendicular to the z - and y -axes. Chlorobenzene has thirty normal modes. As summarized in Table 2 in the column n_{Γ_v} , among these, eleven modes have A_1 symmetry (in-plane vibrations), ten modes have B_2 symmetry (in-plane vibrations), six modes have B_1 symmetry (out-of-plane vibrations) and 3 modes have A_2 symmetry (out-of-plane vibrations). The vibrational mode structure in C_6H_5X molecules has been discussed for quite some time [44–47]. All modes except the A_2 modes are infrared active. The A_1 modes show a -type transitions in the infrared spectra, the B_1 modes c -type transitions and the B_2 modes b -type transitions. Table 1 illustrates the normal modes. The character table for C_{2v} symmetry with the nuclear spin statistical weights is provided in Table 2. As discussed in [29] (for the background see [12,48,26]) the four protons and carbon nuclei exchanged in the permutation $(\alpha\beta)$ correspond with appropriate numbering to $(\alpha\beta) = (26)(35)(2'6')(3'5')$. The total Pauli-allowed species are A^+ and A^- (nurovibronic). The four protons 2, 3, 5, 6 generate a reducible representation D_R in M_{S_4} of the following structure with total nuclear spin I for four protons in parentheses:

$$D_R(I = 2) = 5A^+ \quad (1)$$

$$D_R(I = 1) = 3A^+ + 6B^+ \quad (2)$$

$$D_R(I = 0) = 2A^+ \quad (3)$$

which leads to $D_R(\text{total, four protons}) = 10A^+ + 6B^+$. If this is combined with the 2×4 spin functions of the proton in position 4 and of ^{35}Cl with nuclear spin $I(^{35}\text{Cl}) = 3/2$ and positive parity in position 1 one obtains $D_R(\text{total, all spins}) = 80A^+ + 48B^+$ which leads to the values n_{Γ_s} and the weights g in Table 2. The 128 nuclear spin functions are all of positive parity. Column K_aK_c gives the species of rotational wavefunctions for the corresponding even (e) or odd (o) values of the rotational quantum numbers K_a and K_c . The selection rules for electric dipole transitions are (a) conservation of nuclear spin symmetry and (b) change of parity.

We have measured the FTIR spectrum of chlorobenzene using two different FTIR setups, the nine chamber prototype Bruker spectrometer ZP 2001 ($\Delta\tilde{\nu} = 0.001 \text{ cm}^{-1}$) and the eleven chamber Bruker prototype ETH-SLS 2009 ($\Delta\tilde{\nu} = 0.0008 \text{ cm}^{-1}$) connected to the Swiss Light Source (SLS), in the region 600–900 cm^{-1} as shown by the survey spectrum in Fig. 2. Here we present the rovibrational analysis of the B_1 fundamental band $\tilde{\nu}_{10b} = 741.2240 \text{ cm}^{-1}$ and the A_1 fundamental band $\tilde{\nu}_{12} = 706.6686 \text{ cm}^{-1}$ as well as a slightly improved set of the ground state spectroscopic constants for the isotopomer $C_6H_5^{35}\text{Cl}$.

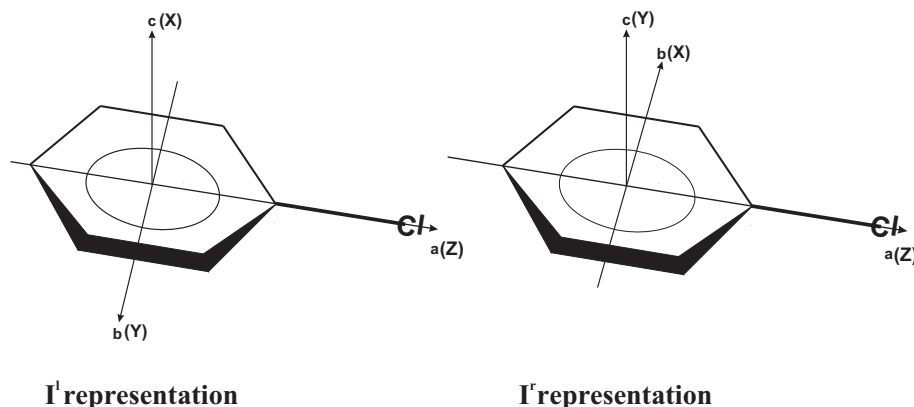


Fig. 1. The structure and the axes systems used for chlorobenzene (schematic, not to scale).

Table 1

Normal modes of chlorobenzene classified into C_{2v} symmetry with A_1, A_2, B_1 and B_2 modes (fundamentals from [35–37] unless otherwise indicated).

35-Chlorobenzene, $C_6H_5^{35}\text{Cl}$					
Mode	Description	$\tilde{\nu}/\text{cm}^{-1}$	Mode	Description	$\tilde{\nu}/\text{cm}^{-1}$
A_1 symmetry			A_2 symmetry		
ν_{20a}	CH stretch	3082	ν_{17a}	CH bend	962
ν_2	CH stretch	3054	ν_{10a}	CH bend	831
ν_{13}	CH stretch	3031	ν_{16a}	CC stretch	403
ν_{8a}	CC stretch	1585			
ν_{19a}	CC stretch	1483.893 ^a			
ν_{7a}	CH stretch	1153			
ν_{9a}	CH bend	1092			
ν_{18a}	CH bend	1025			
ν_1	ring	1003			
ν_{12}	Cl-sensitive	706.6686 ^b			
ν_{6a}	Cl-sensitive	416			
B_2 symmetry			B_1 symmetry		
ν_{20b}	CH stretch	3096	ν_5	CH bend	981
ν_{7b}	CH stretch	3067	ν_{17b}	CH bend	902
ν_{8b}	CC stretch	1598	ν_{10b}	CH bend	741.2239 ^b
ν_{19b}	CC stretch	1448	ν_4	CC twist	685.59 ^b
ν_{14}	CC stretch	1326	ν_{16b}	X-sensitive	467
ν_3	CH bend	1270	ν_{11}	CH bend	200
ν_{9b}	CH bend	1157			
ν_{15}	CH bend	1068			
ν_{6b}	ring	615			
ν_{18b}	Cl-sensitive	293			

^a From [42].

^b This work.

Table 2

Character table for the C_{2v} and $S_2(M_{S_4})$ symmetry groups relating to axes definitions in Fig. 1 (left, as in the I' representation). For the molecular symmetry group $M_{S_4}(\alpha\beta)$ corresponds to the permutation of the equivalent parts of the molecule and the upper right index of the symmetry species indicates parity (+ or -) [26–29]. The symbols have their conventional meaning [1,30], g is the nuclear spin statistical weight for the corresponding rovibronic symmetry.

C_{2v}	$S_2(M_{S_4})$	E	C_2	σ_{xz}	σ_{yz}	μ	J	K_aK_c	n_{Γ_v}	n_{Γ_s}	g
			$(\alpha\beta)$	$(\alpha\beta)^*$	E^*						
A_1	A^+	1	1	1	1	μ_z		ee	11	80	80
A_2	A^-	1	1	-1	-1	J_z		eo	3	0	80
B_1	B^-	1	-1	1	-1	μ_x	J_y	oo	6	0	48
B_2	B^+	1	-1	-1	1	μ_y	J_x	oe	10	48	48

2. Experimental

The FTIR spectrum of chlorobenzene has been first measured with our nine chamber Fourier transform spectrometer Bruker IFS 125 HR Zürich Prototype (ZP) 2001 in the region 600–900 cm^{-1} using an effective resolution of 0.001 cm^{-1} from the

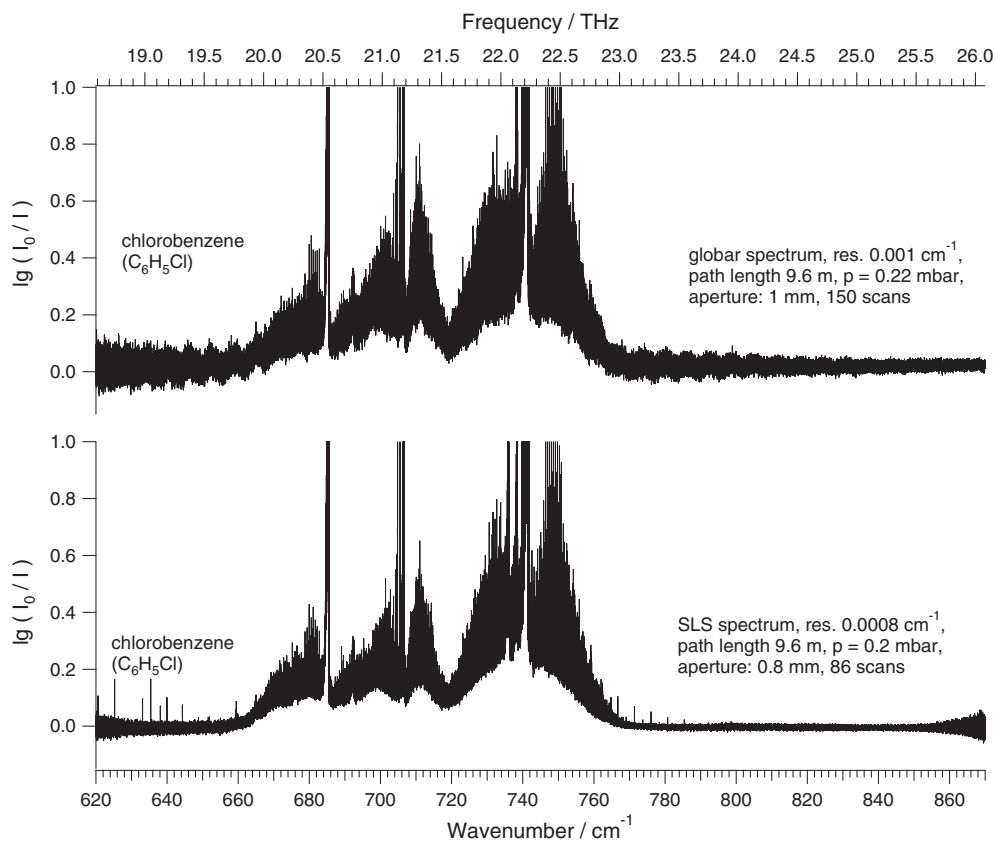


Fig. 2. Overview spectrum of chlorobenzene in the range 620–870 cm^{-1} measured with the 9 chamber system Bruker IFS 120/125 prototype 2001 (upper trace) and the 11 chamber system Bruker IFS 125 ETH-SLS prototype 2009 using synchrotron radiation (lower trace). The significantly lower noise level at a smaller aperture and a much smaller number of scans, shown in the synchrotron spectrum is clearly visible.

measured line width (FWHM) and an aperture of 1 mm. One hundred and fifty spectra were co-added. A White-type cell with a path length ranging from 3.2 m up to 19.2 m was used for the room temperature measurements. The sample pressure was 0.22 mbar. It was measured with a MKS Baratron Type 127. The precise values of the pressure have limited significance because of well-known adsorption effects during a measurement with chlorobenzene.

In order to improve the signal-to-noise ratio and the resolution the same spectral range 600–900 cm^{-1} was measured with our eleven chamber FTIR spectrometer, the ETH-SLS Bruker IFS 125 HR prototype 2009 with the currently worldwide highest available maximum optical path differences of $d_{MOPD} = 11.7$ m which is connected to the infrared port available at the Swiss Light Source (SLS) using sophisticated transfer optics. Here, the synchrotron radiation extracted out of the storage ring is steered along three segments of 1:1 optics using Al coated mirrors kept under vacuum. From the third focal point, the beam is further steered through dedicated transfer optics to the FTIR spectrometer. The transfer optics consist of one parabolic, two toroidal and one flat mirror. The toroidal mirrors are necessary due to the strong astigmatism of the synchrotron radiation. A parallel beam entering the source chamber of the spectrometer gets focused through a parabolic mirror with focal length 41.8 cm to the aperture, which might have a diameter as small as 0.5 mm, and passes on into the interferometer.

The ETH-SLS interferometer of our Bruker prototype spectrometer with $d_{MOPD} = 11.7$ m has at best a resolution of 0.00052 cm^{-1} or 16 MHz. The spectrometer is a further development of our IFS 120/125 prototype 2001 [49,50] which has a $d_{MOPD} = 9.8$ m and a best resolution of 0.0007 cm^{-1} . Further details of our spectrometer have been described in [3,7,8]. We have used an aperture of 0.8 mm leading to an effective resolution of 0.0008 cm^{-1} and again

a White-type cell with a path length ranging from 3.2 m up to 19.2 m for our measurement of chlorobenzene. The pressure measured as described above was 0.2 mbar, and the temperature was 294 K. All spectra were self-apodized. The Doppler width for $\text{C}_6\text{H}_5^{35}\text{Cl}$ at 294 K and 700 cm^{-1} is 0.0008 cm^{-1} which is in the range of our resolution. The spectra were calibrated with OCS (600–900 cm^{-1} , [51]). The significantly lower noise level of the synchrotron spectrum shown in the lower panel of Fig. 2 compared to the spectrum using a global light source and almost twice as many scans shown in the upper panel is clearly visible.

3. Assignment of the fundamentals of $\text{C}_6\text{H}_5^{35}\text{Cl}$ in the range 650–900 cm^{-1}

The 650–775 cm^{-1} region of chlorobenzene shown in Fig. 3 includes two bands with symmetry B_1 and a band with symmetry A_1 labeled as ν_4 (B_1), ν_{12} (A_1) and ν_{10b} (B_1) according to the Wilson notation [52]. The assignment of the observed rovibrational transitions belonging to a particular subband characterized by K_a and K_c series and consisting of P and R branches has been carried out efficiently with an interactive Loomis–Wood (LW) assignment program previously designed for linear [53–55] and quasilinear molecules [56–62] (see also [63]). This graphical pattern recognition and assignment program is a very powerful tool and allows also the assignment of absorption patterns of oblate [64] and prolate [65,66] asymmetric top molecules. Other recent assignment programs of this type include the CAAARS [67], the AABS [68] program packages and the Pgpohr program [69,70] (see also the review and discussion in [63]).

As the Loomis–Wood diagram of the ν_{12} band in the upper part of Fig. 3 illustrates, the a -type structure of this band consisting of

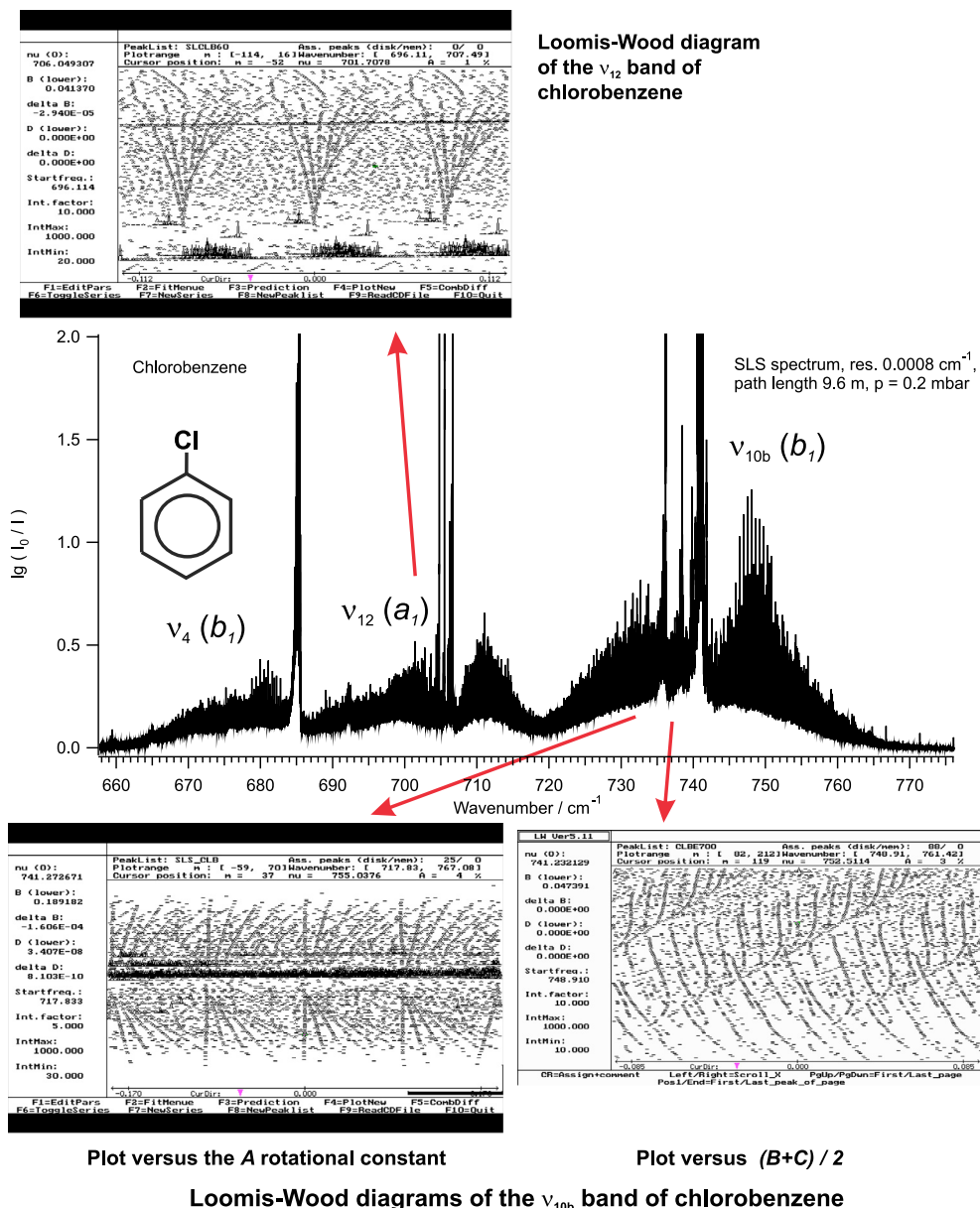


Fig. 3. Overview spectrum of chlorobenzene in the range 650–775 cm^{-1} with the B_1 bands ν_4 and ν_{10b} as well as the A_1 band ν_{12} . The Loomis–Wood diagram of the ν_{12} band shown on the top is plotted versus the C rotational constant. The Loomis–Wood diagrams of the ν_{10b} band of $\text{C}_6\text{H}_5^{35}\text{Cl}$ shown at the bottom of figure are plotted versus the A rotational constant (left) and versus $(B+C)/2$ (right).

K_a series of $\text{C}_6\text{H}_5^{35}\text{Cl}$ is clearly visible and the assignment up to $J \leq 102$ is rather straightforward. A local perturbation for $J \leq 105$ has been identified in the $K_a = 0$ series. The Loomis–Wood diagrams of the ν_{10b} band of $\text{C}_6\text{H}_5^{35}\text{Cl}$ shown at the bottom of Fig. 3 are plotted versus the A rotational constant (left) and versus $(B+C)/2$ (right). Using these two diagrams it was possible to assign this fundamental up to $J \leq 95$, $K_a \leq 35$ and $K_c \leq 66$. However, so far we have not assigned the transitions in the spectrum of the $\text{C}_6\text{H}_5^{37}\text{Cl}$ isotopomer.

4. Results for the spectroscopic parameters and discussion

4.1. Effective Hamiltonian parameters

The rovibrational analysis has been carried out with Watson’s A reduced effective Hamiltonian in the I^r representation (Fig. 1) up to sextic centrifugal distortion constants [71]:

$$\begin{aligned} \hat{H}_{\text{rot}}^{v,v} = & A_v \hat{J}_z^2 + B_v \hat{J}_x^2 + C_v \hat{J}_y^2 - \Delta_J^v \hat{J}^4 - \Delta_{JK}^v \hat{J}^2 \hat{J}_z^2 - \Delta_K^v \hat{J}_z^4 \\ & - \frac{1}{2} \left[(\delta_J^v \hat{J}^2 + \delta_K^v \hat{J}_z^2), (\hat{J}_+^2 + \hat{J}_-^2) \right]_+ + \Phi_J^v (\hat{J}^2)^3 \\ & + \Phi_{JK}^v (\hat{J}^2)^2 \hat{J}_z^2 + \Phi_{KJ}^v \hat{J}^2 \hat{J}_z^4 + \Phi_K^v \hat{J}_z^6 \\ & + \frac{1}{2} \left[(\phi_J^v \hat{J}^2)^2 + \phi_{JK}^v \hat{J}^2 \hat{J}_z^2 + \phi_K^v \hat{J}_z^4, (\hat{J}_+^2 + \hat{J}_-^2) \right]_+ \end{aligned} \quad (4)$$

The angular momentum operators are given by $\hat{J}^2 = \hat{J}_x^2 + \hat{J}_y^2 + \hat{J}_z^2$ and $\hat{J}_\pm = \hat{J}_x \pm i\hat{J}_y$. The I^r representation was chosen to reduce correlations during the fit. It is important to stress that the axis system in the I^r representation is different from the system which we used to determine the symmetry of the normal modes, which would correspond to the I^l representation (Fig. 1).

The spectroscopic data were analyzed using the WANG program described in detail in Ref. [72] (see also [63]). The spectroscopic

constants of each band were fitted separately according to the *A* reduction.

4.2. Rovibrational analysis of the ground state of $C_6H_5^{35}Cl$

The spectroscopic constants of the ground state of $C_6H_5^{35}Cl$ have been determined by submm wave spectroscopy up to $J = 105$ [43] and are listed in Table 3. From the present work 3116 combination differences calculated from the *a*-type transitions of the ν_{12} band and from the *c*-type transitions of the ν_{10b} band of $C_6H_5^{35}Cl$ have been determined and inserted into the least squares adjustment. Only the quartic Δ_K constant needed readjustment. All other constants have been held fixed to the values of [43] as shown in Table 3. As a further check, the combination differences have been calculated with the fixed values of all the parameters from [43]. However, this leads to a $d_{rms} = 0.00063 \text{ cm}^{-1}$ compared to $d_{rms} = 0.00021 \text{ cm}^{-1}$ obtained by adjusting the Δ_K constant. The ground state constants have been held fixed to the values in the third column in Table 3 during the adjustment of the constants of the ν_{12} and ν_{10b} state of $C_6H_5^{35}Cl$.

4.3. Rovibrational analysis of the ν_{12} fundamental of $C_6H_5^{35}Cl$

The adjustment of the spectroscopic constants of the ν_{12} state of $C_6H_5^{35}Cl$ listed in Table 4 have been performed using transitions up to $J \leq 95$. Transitions above this value have not been considered due to the local perturbations. The sextic distortion constants Φ_J , Φ_{JK} and Φ_{KJ} have been determined for ν_{12} . However, during the fit the *A* rotational constant and the quartic constants Δ_{JK} and Δ_K have been held fixed at their values in the ground state. A closer look at the values of the rotational constants *B* and *C* illustrates their small change upon excitation which is on the order of 10^{-5} cm^{-1} and typical of *a*-type transitions. More than 1600 transitions have been included in the least squares adjustment leading to a root mean square deviation $d_{rms} = 2 \times 10^{-4} \text{ cm}^{-1}$. Fixing some of the values of the spectroscopic constants mentioned above was necessary, because of the relatively small number of $K_a \leq 8$ observed subbands. The corresponding lack of data results in strong correlations during the fitting procedure when floating all parameters. The best fit was obtained after several trials by fixing *A*, Δ_{JK} and Δ_K at the ground state values. Alternative fits with floating these parameters as well leads to correlations in particular between *A* and *B*, without any improvement in the d_{rms} . Floating the sextic constants Φ_J , Φ_{JK} and Φ_{KJ} improves the fits presumably

Table 3

Spectroscopic constants in cm^{-1} of the ground state (gs) from [43] and from combination differences calculated from the assignments of the ν_{12} and ν_{10b} states of the $C_6H_5^{35}Cl$ isotopomer in the *A* reduction. We retained the constants of [43] for the ground state except Δ_K which was readjusted in the fit with uncertainties listed as 1σ in parentheses in terms of the last significant digit [30].

<i>A</i>	gs [43]	gs (CD, this work)
$\bar{\nu}_0$ (cm^{-1})	0	0
<i>A</i> (cm^{-1})	0.189207295	0.189207295
<i>B</i> (cm^{-1})	0.052595956	0.052595956
<i>C</i> (cm^{-1})	0.041150963	0.041150963
$\Delta_J/10^{-9} \text{ cm}^{-1}$	2.01156	2.01156
$\Delta_{JK}/10^{-9} \text{ cm}^{-1}$	9.40404	9.40404
$\Delta_K/10^{-9} \text{ cm}^{-1}$	30.28760	29.0600(10)
$\delta_J/10^{-9} \text{ cm}^{-1}$	0.482901	0.482901
$\delta_K/10^{-9} \text{ cm}^{-1}$	10.25510	10.25510
<i>N</i>	183	3116
d_{rms} (cm^{-1})		0.00021
d_{rms} (MHz)	0.061	
J_{max} for fit	105	95

Table 4

Spectroscopic constants in cm^{-1} of the ν_{12} and ν_{10b} states of the $C_6H_5^{35}Cl$ isotopomer in the *A* reduction. Uncertainties listed as 1σ in parentheses in terms of the last significant digit. When no uncertainties are given this parameter was held fixed at the corresponding ground state value.

<i>A</i>	ν_{12}	ν_{10b}
$\bar{\nu}_0$ (cm^{-1})	706.668550(39)	741.223957(32)
<i>A</i> (cm^{-1})	0.189207295	0.189040776(27)
<i>B</i> (cm^{-1})	0.052567056(68)	0.05260956(60)
<i>C</i> (cm^{-1})	0.041118274(32)	0.04116261(71)
$\Delta_J/10^{-9} \text{ cm}^{-1}$	1.875(13)	1.896(11)
$\Delta_{JK}/10^{-9} \text{ cm}^{-1}$	9.40404	9.40404
$\Delta_K/10^{-9} \text{ cm}^{-1}$	29.0600	29.062(20)
$\delta_J/10^{-9} \text{ cm}^{-1}$	0.409(11)	0.196(72)
$\delta_K/10^{-9} \text{ cm}^{-1}$	12.90(27)	4.71(31)
$\Phi_J/10^{-12} \text{ cm}^{-1}$	0.00115(78)	−0.00407(56)
$\Phi_{JK}/10^{-12} \text{ cm}^{-1}$	1.578(62)	0.1650(45)
$\Phi_{KJ}/10^{-12} \text{ cm}^{-1}$	−21.4(12)	−0.1557(55)
<i>N</i>	1625	6340
d_{rms} (cm^{-1})	0.00020	0.00016
J_{max} for fit	95	93

because of perturbations at higher *J* values where ν_4 may act as interacting partner. The parameters obtained from our best fits clearly must be considered as effective fit parameters, which is adequate in such an empirical representation. In an alternative strategy one might consider estimating some of the higher parameters by *ab initio* calculations which seems not really important at the present stage of our analysis.

Using the constants in Table 4 the ν_{12} fundamental of $C_6H_5^{35}Cl$ was simulated as shown in Fig. 4. The upper trace in each panel shows the measured spectrum and the lower trace the simulation. The middle and lower panels are enlargements of parts in the upper panel. As the enlargements in Fig. 4 illustrate, there is good agreement between the measured and simulated $C_6H_5^{35}Cl$ spectrum. Of course, the match is not perfect because numerous hot band transitions indicated by the large number of Q branches visible in the spectrum and the transitions of the $C_6H_5^{37}Cl$ isotopomer have not been considered. The population of the vibrational ground state is only $Q_{vib}^{-1} = 0.251$ at 294 K. On the other hand the quite good agreement between the measured and simulated $C_6H_5^{35}Cl$ spectrum indicates why it was impossible for us to assign a sufficient number of $C_6H_5^{37}Cl$ lines.

4.4. Rovibrational analysis of the ν_{10b} fundamental of $C_6H_5^{35}Cl$

The ν_{10b} band of $C_6H_5^{35}Cl$ is not as perturbed as the ν_{10b} band of phenol [7]. All rotational and quartic distortion constants of the ν_{10b} state of $C_6H_5^{35}Cl$ have been determined (Table 4) except the quartic constant Δ_{JK} which was held fixed at the ground state value. The determination of the sextic constants Φ_J , Φ_{JK} , Φ_{KJ} indicates a possible weak interaction with a dark state. More than 6300 transitions were used in the fitting procedure. The change of the *A* rotational constant upon excitation is larger than those of the *B* and *C* constants as is typical of *c*-type transitions. In any case, both for ν_{10b} and ν_{12} the rotational parameters should be considered as effective fit parameters.

Using the spectroscopic constants shown in Table 4 the ν_{10b} band of $C_6H_5^{35}Cl$ was simulated and is shown (lower trace) together with the experimental spectrum (upper trace) in the upper panel of Fig. 5. Enlargements of the shaded areas in the upper panel are shown in the lower panels of Fig. 5 and in Figs. 6 and 7. Further detailed comparisons of parts of the simulated spectrum of $C_6H_5^{35}Cl$ and the measured chlorobenzene spectrum shown in Fig. 6 and Fig. 7 illustrate the nice agreement between

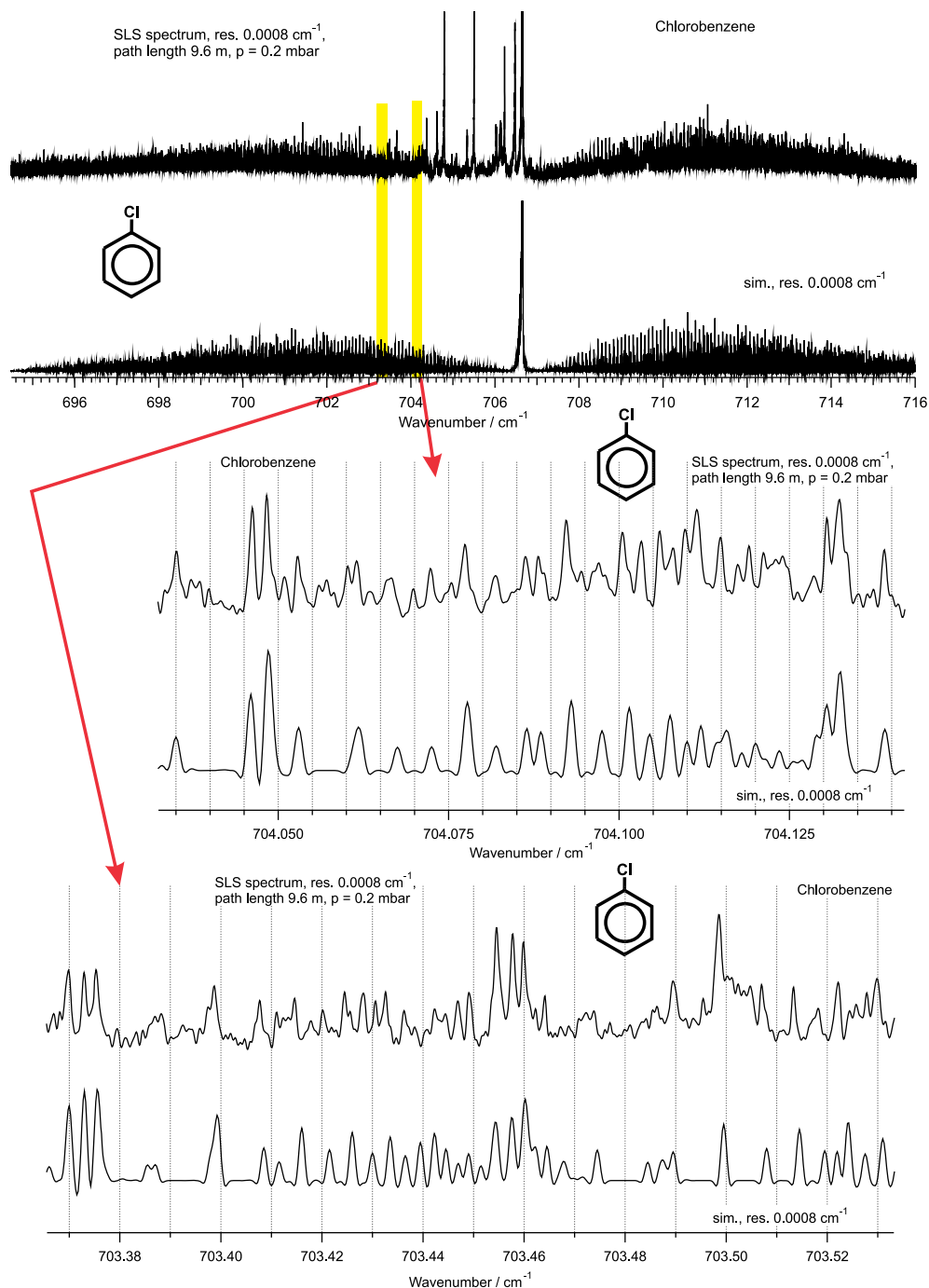


Fig. 4. Measured spectrum (upper trace) of chlorobenzene and simulated spectrum (lower trace) of the ν_{12} fundamental of the $C_6H_5^{35}Cl$ isotopomer are shown in the upper panel. The lower panels show enlargements in the 704.1 cm^{-1} (middle) and 703.44 cm^{-1} (bottom) regions.

measured and simulated spectrum covering the entire spectral range of this band. The agreement is surprisingly good if one takes into account that the hot band lines and the lines of the other isotopomer $C_6H_5^{37}Cl$ are not included in the simulation as already discussed for the ν_{12} fundamental.

5. Conclusions

The rovibrational analysis of the infrared spectra of chlorobenzene at room temperature is an excellent example to illustrate the great advantage of highest resolution FTIR spectroscopy using synchrotron radiation. Due to the high brilliance of the synchrotron

light source it is possible to use apertures as small as 0.8 mm making it possible to apply the full resolution capability of our eleven chamber interferometer. Even spectral features generated by rotational constants as small as 0.05 cm^{-1} can now be resolved and assigned.

We were able to rotationally resolve the infrared spectra of chlorobenzene at room temperature in the region $620\text{--}900\text{ cm}^{-1}$. The assignment of the rovibrational lines of the isotopomer $C_6H_5^{35}Cl$ is straightforward due to the highly resolved spectra. The ν_{10b} fundamental of $C_6H_5^{35}Cl$ was analyzed up to $J \leq 95$. The ν_{12} fundamental of $C_6H_5^{35}Cl$ was analyzed up the crossing region. However, an assignment of the $C_6H_5^{37}Cl$ transitions in both fundamentals is quite challenging due to the lower intensity and the

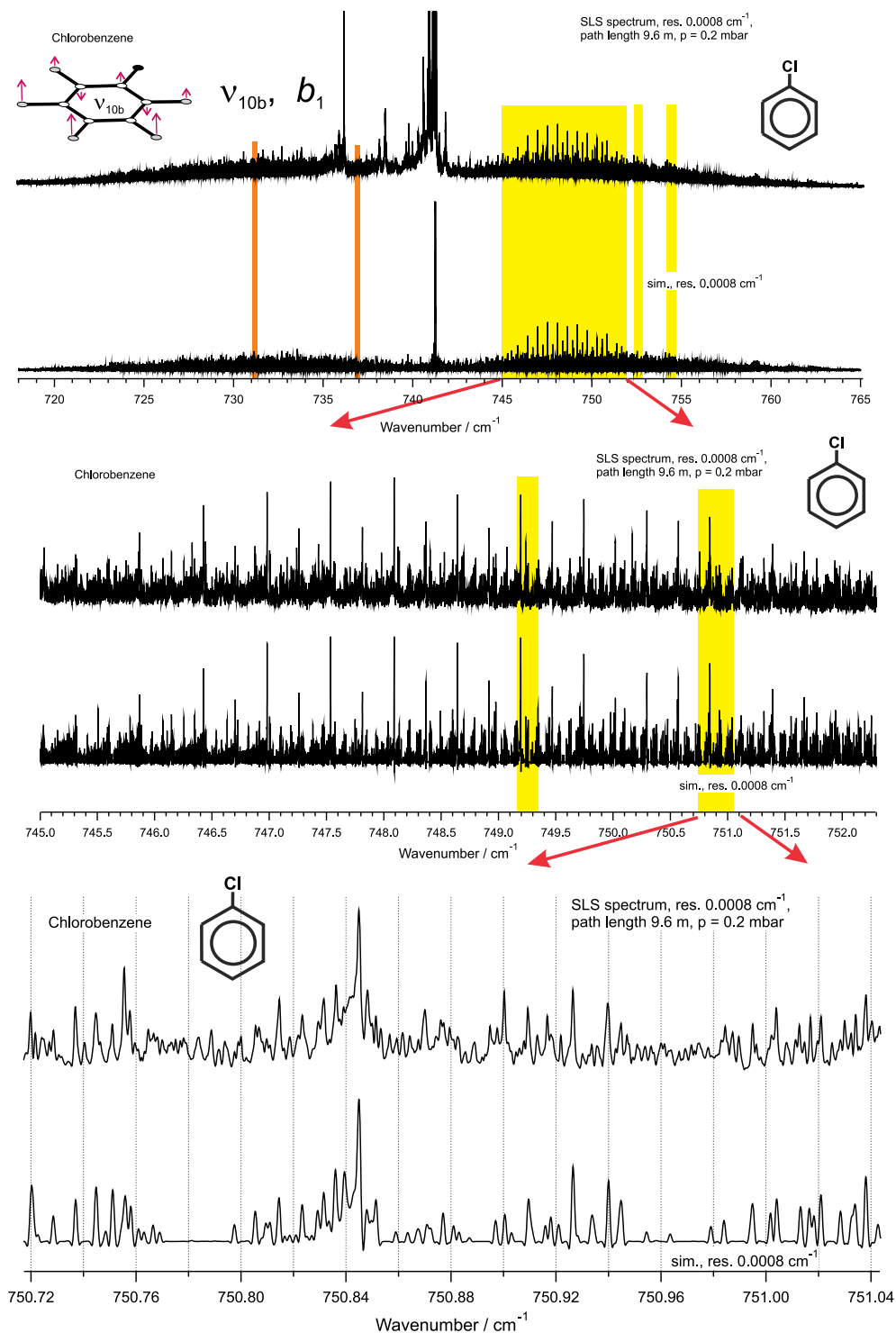


Fig. 5. Measured spectrum (upper trace) of chlorobenzene and simulated spectrum (lower trace) of the ν_{10b} fundamental of the $C_6H_5^{35}Cl$ isotopomer are shown in the upper panel. The lower panels show enlargements in the 749 cm^{-1} (middle) and 750.88 cm^{-1} (bottom) regions.

presence of hot band lines. To detect and identify $C_6H_5^{37}Cl$ absorption lines it might be helpful to cool the spectra down in order to minimize the hot band transitions or else one might use isotopically enriched samples of this isotopomer.

Our analysis of chlorobenzene's FTIR spectrum is a further extension of our project to understand the dynamics and spectroscopy of aromatic systems. Compared to the complicated FTIR spectra of fluorobenzene [33,41], pyridine [50], pyrimidine [64], indole, naphthalene [3], azulene [8] and phenol [7] the

chlorobenzene spectra are relatively easy to understand as long as the lines are resolved. No complicated resonance features have been detected.

A comparison of the FTIR spectra of the aromatic molecules monodeutero-benzene, $^{13}C^{12}C_5H_6$ [38–40], fluorobenzene [33,41] and chlorobenzene, all of C_{2v} symmetry show similar structures for the out-of-plane modes (c -type bands), but they look completely different with regard to the in-plane modes (a -type bands). The complicated band structure of fluorobenzene around 800 cm^{-1}

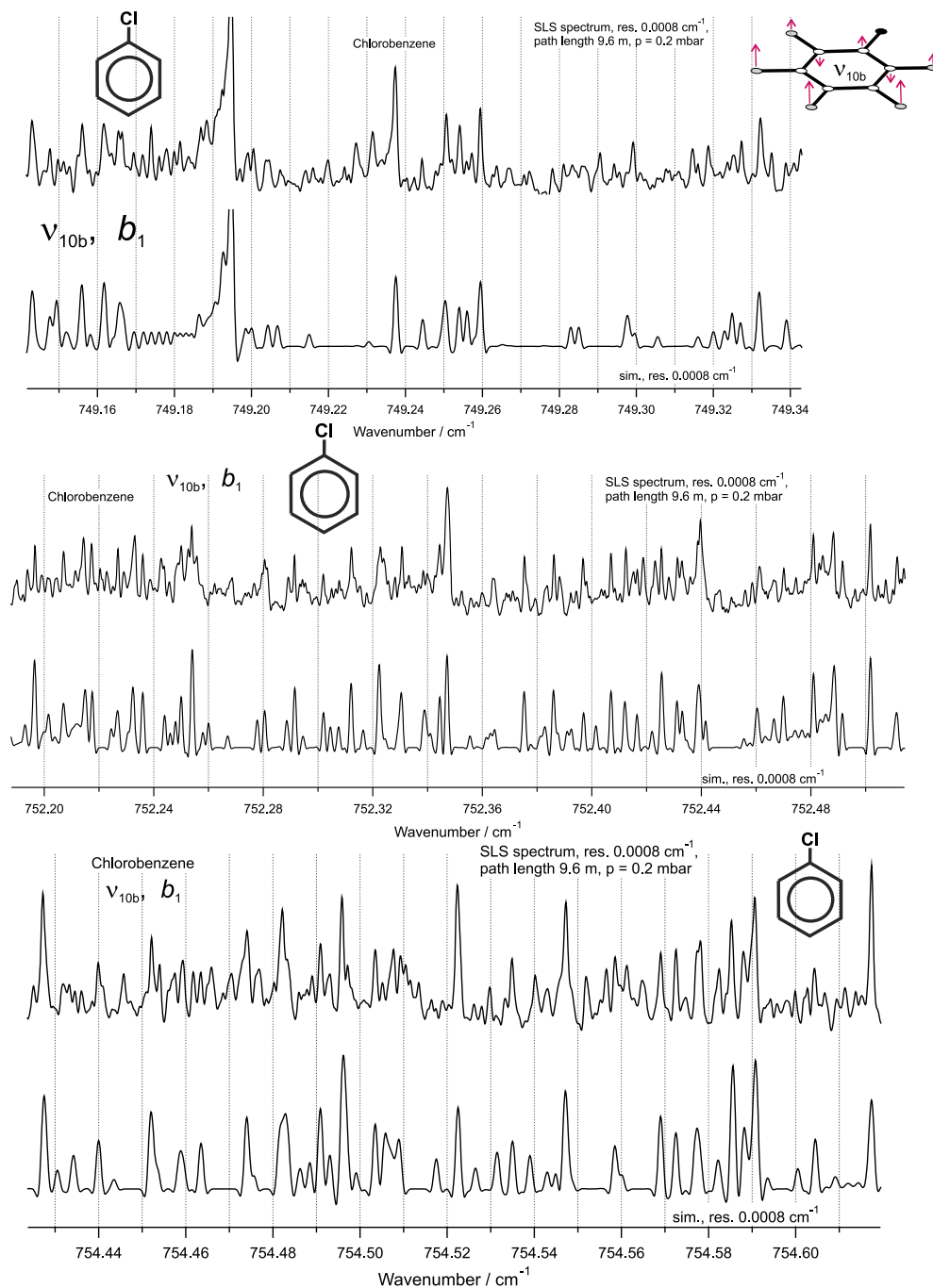


Fig. 6. Enlargements of the shaded areas around 749.26 cm^{-1} (upper panel), 752.36 cm^{-1} (middle panel) and 754.52 cm^{-1} (lower panel) from the upper panel of Fig. 5. The measured spectrum of the ν_{10b} fundamental of chlorobenzene is shown in the upper trace and the simulated spectrum of the ν_{10b} fundamental of the $\text{C}_6\text{H}_5^{35}\text{Cl}$ isotopomer in the lower trace.

is missing for chlorobenzene. The ν_{12} band part of the resonance structure in fluorobenzene is shifted to 707 cm^{-1} in chlorobenzene.

The present results and detailed analysis should be useful in identifying regions where chlorobenzene can be detected spectroscopically as a pollutant even given the overlap with CO_2 absorptions in this range. Benzene and substituted benzene derivatives have also been prototypes in studies of intramolecular vibrational redistribution [73–75] and in this context the present high resolution analysis can provide a starting point for the study of vibrational and rovibrational interactions in more highly excited levels of chlorobenzene.

Our work also demonstrates the capabilities of rovibrational “eigenstate-resolved” analyses for relatively complex aromatic molecules using synchrotron-based FTIR spectroscopy which can be extended towards the analysis of spectra of chiral ring compounds [76] [33]. Here such line-resolved analyses are a crucial first step towards experiments on molecular parity violation [11–15].

Acknowledgments

Our work is supported financially by the Schweizerischer Nationalfonds, ETH Zurich, Paul-Scherrer-Institute and European

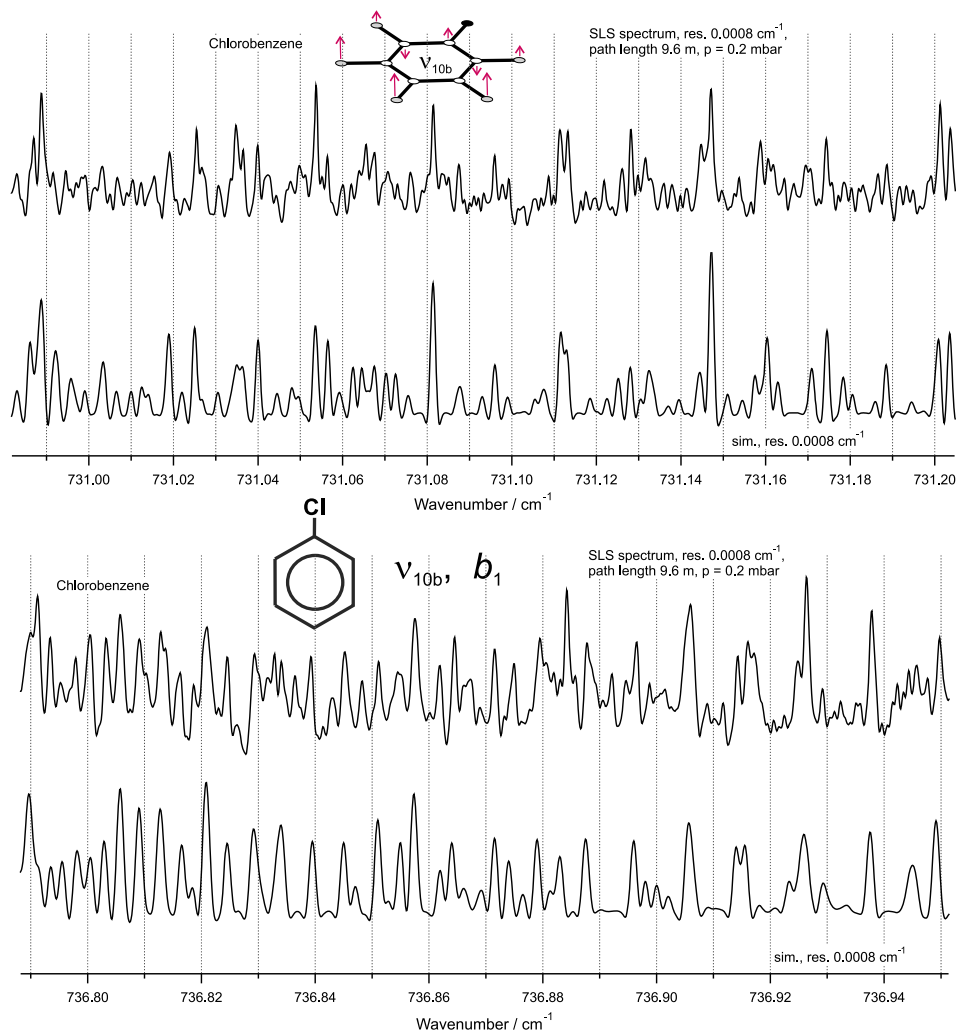


Fig. 7. Enlargement of the shaded areas around 731.08 cm^{-1} (upper panel) and 736.86 cm^{-1} (lower panel) from the upper panel of Fig. 5. The measured spectrum of the ν_{10b_1} fundamental of chlorobenzene is shown in the upper trace and the simulated spectrum of the ν_{10b_1} fundamental of the $\text{C}_6\text{H}_5^{35}\text{Cl}$ isotopomer in the lower trace.

Research Council by an Advanced Grant. The research leading to these results has also received funding from the European Union's Seventh Framework Programme (FP7/2007-20013) ERC Grant Agreement No. 290925.

Appendix A

Table of line frequencies deposited as 126 pages of [supporting information](#). The tables of line frequencies [77] provide the ground state combination differences (Table A1), the rovibrational line frequencies for ν_{12} (Table A2) and for ν_{10b_1} (Table A3).

Appendix B. Supplementary material

Supplementary data associated with this article can be found, in the online version, at <http://dx.doi.org/10.1016/j.jms.2015.03.004>.

References

- [1] S. Albert, K. Keppler Albert, M. Quack, *High Resolution Fourier Transform Infrared Spectroscopy*, in: M. Quack, F. Merkt (Eds.), *Handbook of High Resolution Spectroscopy*, vol. 2, Wiley, John Wiley & Sons Ltd., 2011, pp. 965–1019 (Chapter 26).
- [2] A.R.W. McKellar, *J. Mol. Spectrosc.* 262 (1) (2010) 1–10.
- [3] S. Albert, K.K. Albert, P. Lerch, M. Quack, *Faraday Discuss.* 150 (2011) 71–99.
- [4] M.K. Bane, C.D. Thompson, E.G. Robertson, D.R.T. Appadoo, D. McNaughton, *Phys. Chem. Chem. Phys.* 13 (15) (2011) 6793–6798.
- [5] O. Pirali, M. Goubet, T.R. Huet, R. Georges, P. Soulard, P. Asselin, J. Courbe, P. Roy, M. Vervioet, *Phys. Chem. Chem. Phys.* 15 (25) (2013) 10141–10150.
- [6] Z. Chen, J. van Wijngaarden, *J. Phys. Chem. A* 116 (38) (2012) 9490–9496.
- [7] S. Albert, P. Lerch, R. Prentner, M. Quack, *Angew. Chem. Int. Ed. (Engl.)* 52 (2013) 346–349.
- [8] S. Albert, P. Lerch, M. Quack, *ChemPhysChem* 14 (14) (2013) 3204–3208.
- [9] S. Albert, S. Bauerecker, K. Keppler, P. Lerch, M. Quack, *Synchrotron based FTIR spectroscopy of chiral molecules CDBrClF and CHBr IF*, in: D. Stock, R. Wester, R. Scheier (Eds.), *Proceedings of the 19th Symposium on Atomic, Cluster and Surface Physics (SASP 2014)*, University Center Obergurgl, Austria, 8th to 14th February 2014, Innsbruck University Press, Innsbruck, 2014, pp. 152–155. ISBN: 978-3-902936-26-4.
- [10] S. Albert, P. Lerch, M. Quack, A. Wokaun, *High resolution FTIR spectroscopy of indene (C_9H_8) with synchrotron radiation*, in: D. Stock, R. Wester, R. Scheier (Eds.), *Proceedings of the 19th Symposium on Atomic, Cluster and Surface Physics (SASP 2014)*, University Center Obergurgl, Austria, 8th to 14th February 2014, Innsbruck University Press, Innsbruck, 2014, pp. 240–243. ISBN: 978-3-902936-26-4.
- [11] S. Albert, M. Quack, *Nachr. Chem.* 62 (2014) 313–318.
- [12] M. Quack, *Fundamental symmetries and symmetry violations from high resolution spectroscopy*, in: M. Quack, F. Merkt (Eds.), *Handbook of High Resolution Spectroscopy*, vol. 1, John Wiley & Sons Ltd., Chichester, New York, 2011, pp. 659–722 (Chapter 18).
- [13] M. Quack, *Angew. Chem. Int. Ed. (Engl.)* 41 (2002) 4618–4630.
- [14] M. Quack, *Eur. Rev.* 22 (SupplementS1) (2014) S50–S86.
- [15] M. Quack, *On biomolecular homochirality as a quasi-fossil of the evolution of life*, in: S.A. Rice, A.R. Dinner (Eds.), *Advances in Chemical Physics: Proceedings of the 240 Conference: Science's Great Challenges*, vol. 157, John Wiley & Sons Ltd., 2014, pp. 249–290 (Chapter 17).
- [16] J.-M. Flaud, J. Orphal, *Spectroscopy of the Earth's atmosphere*, in: M. Quack, F. Merkt (Eds.), *Handbook of High Resolution Spectroscopy*, vol. 3, John Wiley & Sons Ltd., Chichester, 2011, pp. 1971–1992 (Chapter 57).

- [17] A. Barbe, P. Marche, C. Secroun, P. Jouve, *Geophys. Res. Lett.* 6 (6) (1979) 463–465.
- [18] A. Barbe, M.R. De Backer-Barilly, V.G. Tyuterev, S. Kassi, A. Campargue, J. Mol. Spectrosc. 269 (2) (2011) 175–186.
- [19] J.M. Flaud, C. Camy-Peyret, A. Barbe, C. Secroun, P. Jouve, *J. Mol. Spectrosc.* 80 (1) (1980) 185–199.
- [20] O.N. Ulenikov, E.S. Bekhtereva, S. Albert, S. Bauerecker, H.M. Niederer, M. Quack, *J. Chem. Phys.* 141 (23) (2014) 234302.
- [21] S. Albert, S. Bauerecker, V. Boudon, L. Brown, J.-P. Champion, M. Loëte, A. Nikitin, M. Quack, *Chem. Phys.* 356 (1–3) (2009) 131–146.
- [22] A.V. Nikitin, V. Boudon, C. Wenger, S. Albert, L.R. Brown, S. Bauerecker, M. Quack, *Phys. Chem. Chem. Phys.* 15 (25) (2013) 10071–10093.
- [23] H.-M. Niederer, X.-G. Wang, T. Carrington Jr, S. Albert, S. Bauerecker, V. Boudon, M. Quack, *J. Mol. Spectrosc.* 291 (2013) 33–47.
- [24] V. Boudon, J.-P. Champion, T. Gabard, M. Lote, M. Rotger, C. Wenger, *Spherical top theory and molecular spectra*, in: M. Quack, F. Merkt (Eds.), *Handbook of High Resolution Spectroscopy*, vol. 3, John Wiley & Sons Ltd., Chichester, 2011, pp. 1437–1460 (Chapter 39).
- [25] S. Albert, S. Bauerecker, M. Quack, A. Steinlin, *Mol. Phys.* 105 (5) (2007) 541–558.
- [26] M. Quack, *Mol. Phys.* 34 (2) (1977) 477–504.
- [27] K.V. Puttkamer, M. Quack, *Mol. Phys.* 62 (5) (1987) 1047–1064.
- [28] K.V. Puttkamer, M. Quack, M.A. Suhm, *Mol. Phys.* 65 (5) (1988) 1025–1045.
- [29] E. Riedle, A. Beil, D. Luckhaus, M. Quack, *Mol. Phys.* 81 (1) (1994) 1–15.
- [30] E.R. Cohen, T. Cvitas, J.G. Frey, B. Holstrom, K. Kuchitsu, R. Marquardt, I. Mills, F. Pavese, M. Quack, J. Stohner, H.L. Strauss, M. Takami, A.J. Thor, *Quantities, Units and Symbols in Physical Chemistry*, The Royal Society of Chemistry, 2011 (3rd revised printing). <http://dx.doi.org/10.1039/9781847557889>.
- [31] B. Johnke, D. Menke, J. Böske, *WHO Revision of the toxic equivalency factors for dioxins and furans and its impact on the emission of waste incineration plants in Germany*, vol. 31, *Newsletter of the WHO Collaborating Center for Air Quality Management and Air Pollution Control*, Berlin, 2003, p. 5.
- [32] W. Saudermann, *Naturwissenschaften* 61 (5) (1974) 207–213.
- [33] S. Albert, M. Quack, *High resolution infrared spectroscopy of aromatic compounds*, in: V. Grill, T.D. Märk (Eds.), *Contributions, 15th Symposium on Atomic and Surface Physics and Related Topics, Obergurgl, Österreich, 4. – 9.2.2006*, Innsbruck University Press, ISBN: 3-901249-82-6, Innsbruck, 2006, pp. 213 – 216.
- [34] D.H. Whiffen, *J. Chem. Soc.* 1956 (1956) 1350–1356.
- [35] H.D. Bist, V.K. Sarin, A. Ojha, Y.S. Jain, *Spectrochim. Acta Part A: Mol. Spectrosc.* 26 (4) (1970) 841–847.
- [36] H.D. Bist, V.N. Sarin, A. Ojha, Y.S. Jain, *Appl. Spectrosc.* 24 (1970) 292–294.
- [37] Y.S. Jain, H.D. Bist, *J. Mol. Spectrosc.* 47 (1) (1973) 126–133.
- [38] M. Snels, H. Hollenstein, M. Quack, E. Cané, J. Miani, A. Trombetti, *Mol. Phys.* 100 (2002) 981–1001.
- [39] M. Snels, A. Beil, H. Hollenstein, M. Quack, *Chem. Phys.* 225 (1997) 107–130.
- [40] H. Hollenstein, S. Piccirillo, M. Quack, M. Snels, *Mol. Phys.* 71 (4) (1990) 759–768.
- [41] S. Albert, K. Keppler, M. Quack, *Mol. Phys.* (2015), <http://dx.doi.org/10.1080/00268976.2015.1023754>. in press.
- [42] A. Uskola, F.J. Basterretxea, F. Castano, *J. Mol. Spectrosc.* 202 (2) (2000) 262–271.
- [43] Z. Kisiel, *J. Mol. Spectrosc.* 144 (2) (1990) 381–388.
- [44] N. Fuson, C. Garrigou-Lagrange, M.L. Josien, *Spectrochim. Acta* 16 (1–2) (1960) 106–127.
- [45] E.W. Schmid, J. Brandmüller, G. Nonnenmacher, *Z. Elektrochem. Bericht. Bunsengesellschaft phys. Chem.* 64 (5) (1960) 726–733.
- [46] W.D. Mross, G. Zundel, *Spectrochim. Acta Part A: Mol. Spectrosc.* 26 (5) (1970) 1097–1107.
- [47] G. Herzberg, *Molecular Spectra and Molecular Structure, II. Infrared and Raman Spectra of Polyatomic Molecules*, Krieger Publishing Company, Malabar Florida, USA, 1991.
- [48] H.C. Longuet-Higgins, *Mol. Phys.* 6 (5) (1963) 445–460.
- [49] S. Albert, K.K. Albert, M. Quack, *Trends Opt. Photon.* 84 (2003) 177–180.
- [50] S. Albert, M. Quack, *ChemPhysChem* 8 (2007) 1271–1281, <http://dx.doi.org/10.1002/cphc.200700018>.
- [51] A. Maki, J.S. Wells, *Wavenumber Calibration Tables from Heterodyne Frequency Measurements*, NIST Special Publication 821, USA, 1991.
- [52] E.B. Wilson, *Phys. Rev.* 45 (1934) 706–714.
- [53] A. Maki, W. Quapp, S. Klee, G.C. Mellau, S. Albert, *J. Mol. Spectrosc.* 174 (2) (1995) 365–378.
- [54] A. Maki, W. Quapp, S. Klee, G.C. Mellau, S. Albert, *J. Mol. Spectrosc.* 180 (2) (1996) 323–336.
- [55] A. Maki, W. Quapp, S. Klee, G.C. Mellau, S. Albert, *J. Mol. Spectrosc.* 185 (1997) 356–369.
- [56] B.P. Winnewisser, J. Reinstädler, K.M.T. Yamada, J. Behrend, *J. Mol. Spectrosc.* 136 (1989) 12–16.
- [57] W. Quapp, S. Albert, B.P. Winnewisser, M. Winnewisser, *J. Mol. Spectrosc.* 160 (2) (1993) 540–553.
- [58] S. Albert, M. Winnewisser, B.P. Winnewisser, *Ber. Bunsenges. Phys. Chem.* 100 (1996) 1876–1896.
- [59] S. Albert, M. Winnewisser, B.P. Winnewisser, *Microchim. Acta* 14 (1997) 79–88.
- [60] S. Albert, M. Winnewisser, B.P. Winnewisser, *Ber. Bunsenges. Phys. Chem.* 101 (1997) 1165–1186.
- [61] S. Albert, K. Albert, M. Winnewisser, B.P. Winnewisser, *Ber. Bunsenges. Phys. Chem.* 102 (1998) 1428–1448.
- [62] S. Albert, M. Winnewisser, B.P. Winnewisser, *J. Mol. Struct.* 599 (2001) 347–369.
- [63] S. Albert, K. Keppler Albert, H. Hollenstein, C. Manca Tanner, M. Quack, *Fundamentals of rotation-vibration spectra*, in: M. Quack, F. Merkt (Eds.), *Handbook of High-Resolution Spectroscopy*, vol. 1, John Wiley & Sons Ltd., Chichester, 2011, pp. 117–173 (Chapter 3).
- [64] S. Albert, M. Quack, *J. Mol. Spectrosc.* 243 (2007) 280–291, <http://dx.doi.org/10.1016/j.jms.2007.04.009>.
- [65] S. Albert, K. Albert, M. Quack, *J. Mol. Struct.* 695–696 (2004) 385–394.
- [66] S. Albert, H. Hollenstein, M. Quack, M. Willeke, *Mol. Phys.* 104 (16–17) (2006) 2719–2735, <http://dx.doi.org/10.1080/00268970600828991>.
- [67] I.R. Medvedev, M. Winnewisser, B.P. Winnewisser, F.C. De Lucia, E. Herbst, *J. Mol. Struct.* 742 (1–3) (2005) 229–236.
- [68] Z. Kisiel, L. Pszczolkowski, I.R. Medvedev, M. Winnewisser, F.C. De Lucia, E. Herbst, *Rotational spectrum of trans-trans diethyl ether in the ground and three excited vibrational states*, *J. Mol. Spectrosc.* 233 (2005) 231–243.
- [69] C.M. Western, P. Gopher, *A Program for Simulating Rotational Structure!*, Website, 1999. <<http://pgopher.chm.bris.ac.uk>>.
- [70] C.M. Western, *PGOPHER, A Program for Simulating Rotational Structure!*, University of Bristol Research Data Repository, Bristol, 2014.
- [71] J.K.G. Watson, *Aspects of quartic and sextic centrifugal effects on rotational energy levels*, in: J. Durig (Ed.), *Vibrational Spectra and Structure*, vol. 6, Elsevier, Amsterdam, 1978, pp. 1–89.
- [72] D. Luckhaus, M. Quack, *Mol. Phys.* 68 (3) (1989) 745–758.
- [73] M. Quack, W. Kutzelnigg, *Ber. Bunsenges. Phys. Chem.* 99 (3) (1995) 231–245.
- [74] R. Marquardt, M. Quack, *Energy redistribution in reacting systems*, in: J. Moore, N. Spencer (Eds.), *Encyclopedia of Chemical Physics and Physical Chemistry (Fundamentals)*, vol. 1, IOP Publ., Bristol, 2001, pp. 897–936 (Chapter A.3.23).
- [75] M. Quack, *Chimia* 55 (2001) 753–758.
- [76] M. Quack, J. Stohner, M. Willeke, *Annu. Rev. Phys. Chem.* 59 (2008) 741–769.
- [77] The line tables of Appendix A have been deposited.